Pergamon

Journal of Structural Geology, Vol. 17, No. 3, pp. 397 to 408, 1995

0191-8141/95 $9.50+0.00

0191-8141(94)00063-8

Geometry, classification and kinematics of *S–C* and *S–C′* fabrics in the Mushandike area, Zimbabwe

TOM G. BLENKINSOP

Department of Geology, University of Zimbabwe, P.O. Box MP 167, Mount Pleasant, Harare, Zimbabwe

and

PETER J. TRELOAR

School of Geological Sciences, Kingston University, Penrhyn Road, Kingston-upon-Thames, Surrey, U.K.

(*Received* 5 *January* 1994; *accepted in revised form* 5 *May* 1994)

Abstract—Planar fabrics in small dextral shear zones in the Mushandike area of the Zimbabwe Archaean craton consist of a sigmoidal primary foliation *S* displaced by discrete shears *C* or *C′*. These planar fabrics can be divided into *porphyroclastic*, *megacrystic* and *banded types*, depending mainly on the values of the angles between *S*- and *C*- or *C′*-surfaces, the structures that define *S*-surfaces, and the spacing of *C*- or *C′*-surfaces. The values of the angles between the foliations are proposed as the basis for a general classification of planar fabrics in shear zones. The values of the angles depend on microstructures and strain. Microstructural evidence shows that slip did not occur on *S*-surfaces, but only on *C*- or *C′*-surfaces. A model for the development of the fabrics proposes that *S*-surfaces lie parallel to the *XY* plane of the local finite strain ellipsoid in domains of simple shear between *C*- or *C′*-surfaces. *C′*-surfaces may form in the orientation of a Coulomb failure surface. The field evidence suggests that an increase in bulk strain is at least partly accommodated by an increase in local strain in domains between *C*- or *C′*-surfaces as the *S*-surfaces rotate with the local finite strain ellipsoid.

INTRODUCTION

Many shear zones contain two planar fabrics that can be divided into a sigmoidal penetrative foliation, and discrete planar shears that displace the foliation. The sigmoidal foliation is often referred to as an *S*-foliation, and the slip surfaces or shears as *C*- or *C′*-surfaces (Berthé *et al.* 1979), extensional crenulation cleavage or *ecc* (Platt & Vissers 1980), shear bands or shear planes (White *et al.* 1980, Simpson 1986), or normal-slip crenulations (Dennis & Secor 1987, 1990). The essential features of these foliations are shown in Fig. 1, which is also used to define the angular relationships between them. Angle α is defined as that between the shear plane and the local orientation of *S*-surfaces between *C*- or *C′*-surfaces, and angle β is that between the shear plane and

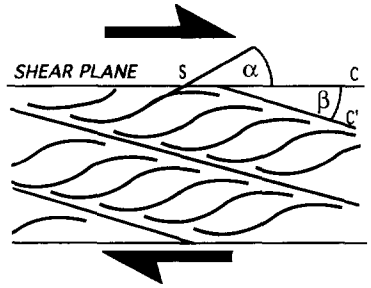

Fig. 1. Schematic diagram of planar fabrics in shear zones. α is the angle between the shear plane and *S*-surfaces, β is the angle between the shear plane and *C′*-surfaces.

C′-surfaces, which are inclined in the opposite direction to the *S*-surfaces. *C*-surfaces are parallel to the shear plane. In addition an angle δ can be defined, which is the angle between *S*- and *C*- or *C′*-surfaces. δ is equal to α between *S*- and *C*-surfaces, and $\delta = \alpha + \beta$ between *S*- and *C′*-surfaces. The examples given below demonstrate that these angles are a useful basis for the classification of the fabrics in this study and others in the literature, and that the angles depend on the pre-deformational microstructure and strain.

Several theories for the origin and evolution of planar fabrics in shear zones have been proposed (e.g. Ramsay 1967, 1980, Berthé *et al.* 1979, Platt & Vissers 1980, Lister & Snoke 1984, Platt 1984, Dennis & Secor 1987, 1990). The theories have contradictory implications for relationships between the bulk strain ellipsoid and the foliations, and predict different values of α, β and δ. For example, *S*-surfaces are proposed as forming parallel to the *XY* plane of the finite strain ellipsoid in simple shear by Ramsay (1967, 1980), Berthé *et al.* (1979) and Lister & Snoke (1984), and therefore cannot be shear surfaces. However, Platt (1984) suggested that slip could occur along *S*-surfaces due to strain partitioning, while Dennis & Secor (1987, 1990) propose that *S*-surfaces are shear planes that are kinematically compatible with 'normal slip crenulations', equivalent to *C′*-surfaces. The question of whether shear occurs on *S*-surfaces is particularly significant in distinguishing both theories and observations on *S–C* and *S–C′* fabrics. Planar fabrics in shear

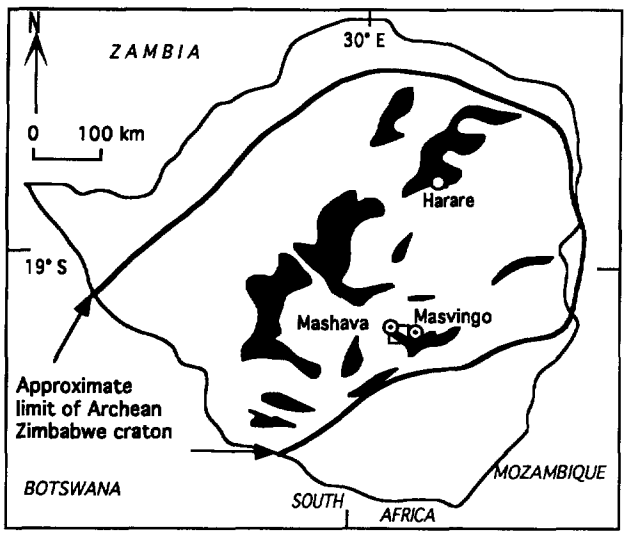

Fig. 2. Location map of the study area in the Archaean Zimbabwe craton. The small box between Mashava and Masvingo is the area of the top half of Fig. 3. Black areas are greenstone belts.

zones have also been investigated by a number of experiments (e.g. Wilson 1984, Shimamoto 1989, Williams & Price 1990), which reveal the development of the foliations with strain particularly well. Understanding the formation of these foliations is important because they are widely used for determining shear sense (e.g. Simpson & Schmid 1983, Simpson 1986), although complications in their use as kinematic indicators have been pointed out by Behrmann (1987).

A network of small shear zones that contain two foliations is exposed in and around the Mushandike granite in the Zimbabwe Archaean craton (Figs. 2 and 3). The shear zone fabrics are exceptionally well-developed, and have a variety of forms. The shear zones therefore provide an excellent opportunity to test the theories mentioned above. We aim to describe and classify shear zone fabrics formed during Archaean deformation of the Mushandike area, to compare them with other examples, and to compare different models for the development of the fabrics in the light of the field observations. These results may have wide significance because the fabrics described here are similar to some other published descriptions.

GEOLOGICAL BACKGROUND

The Mushandike 'granite' covers an area of 132 km^2 between Mashava and Masvingo in the south part of the Zimbabwe Archaean craton (Fig. 2). It is a fairly homogeneous, medium-grained granodiorite–tonalite, but there are significant variations in K-feldspar content, and inclusions of older gneiss (Wilson 1968). The granite has been dated at 2917 ± 171 Ma and 2946 ± 134 Ma by Rb–Sr and Pb–Pb methods respectively (Moorbath *et al.* 1987). Basic metavolcanics and metasediments of the Bulawayan Group in the Mashava–Masvingo greenstone belt with presumed ages of 2.7 Ga. overlie the granite unconformably, and a number of amphibolite dykes belonging to the Mashaba Igneous Complex, thought to be the remains of a magma chamber that fed the overlying Bulawayan group volcanics, cut parts of the Mushandike granite. The granite is intruded at its northeast corner by a younger granite belonging to the Chilimanzi suite of granites which have ages of 2.6 Ga. (Wilson 1990).

Part of the southern margin of the Mushandike granite, together with Bulawayan metasediments and volcanics, are deformed within the Jenya-Mushandike dislocation zone (JMDZ) (Wilson 1990). This is a major regional structure over 100 km long, which to the west, comprises the Jenya fault system, and to the east, south of the Mushandike granite, consists of the Mushandike shear zone (MSZ). The structural geology of the Mushandike area is dominated by two features. First is the Mushandike shear zone itself, characterized by ESE (110°) striking linear and planar fabrics. Second, to the north of the MSZ are located a series of curved shear zones, mostly dextral, which are convex to the south. These shear zones contain similar structures to those of the MSZ and probably developed at the same time as penetrative dextral strike-slip movement on the MSZ (Blenkinsop *et al.* 1990).

Where the shear zones cut granite or siliceous metasedimentary units they contain muscovite as a fabric defining phase. Similarly, where they cut amphibolitic units they carry a recrystallized chlorite-free assemblage with albitic plagioclases and sodic-poor actinolite–tremolite amphiboles. These assemblages imply that shearing was under upper greenschist facies conditions. Shearing probably occurred in the late Archaean (Blenkinsop *et al.* 1990).

SHEAR ZONE GEOMETRY

The curved shear zones located to the north of the MSZ consist of segments of one to a few hundred meters length, which may be aligned or in en échelon geometries to a total of 1 km in length. The shear zone orientation changes systematically from north to south towards the MSZ. In the north, shear zones strike between N and NE, but towards the south, the strike changes to NE–ESE, so that shear zones become subparallel to the ESE-striking MSZ and merge with it. Within the southernmost shear zones, *C'*-shears, with dextral displacement senses, parallel the strike of the MSZ. Shear zones have vertical or sub-vertical dips. The density of shear zones increases towards the MSZ (Fig. 3). Shear senses have been determined for the shear zones on the basis of foliation geometries, asymmetrical porphyroclasts, displaced dykes and small displaced quartz veins. By far the majority of shear zones are dextral, but about 10% are sinistral (Fig. 3). These have more N-strikes and are concentrated in the north of the granite. The sinistral shear zones are considered to have formed in a conjugate orientation to the dextral shear zones by Blenkinsop *et al.* (1990).

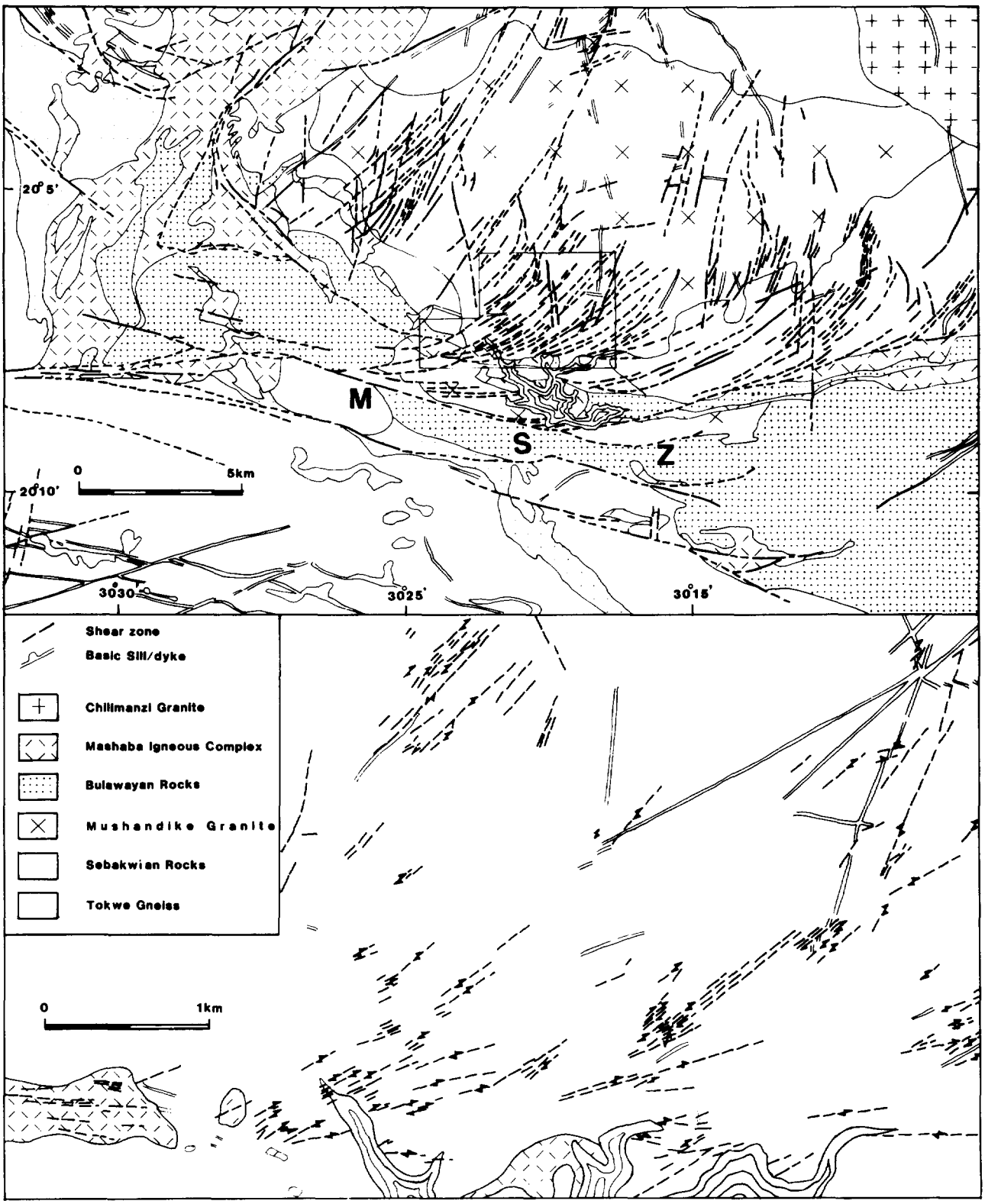

Fig. 3. Shear zones in the Mushandike granite. MSZ—Mushandike shear zone. The lower half of the figure is a detailed map of the boxed area in the centre of the top half. Concentric contours show the area of Mushandike reservoir. Mapping based on Wilson (1968), Dhilwayo (1990), Muranda (1990) and the authors.

SHEAR ZONE FABRICS

Measurement of the angles α and β present some practical difficulties. The orientations of *S*-,*C*- and *C'*-surfaces can be measured with the accuracy of the compass-clinometer ($\pm 1°$): δ can then be calculated to this accuracy. The strike and dip of the shear zones can be estimated to $\pm\sim 5°$ on the outcrop, which gives a lower accuracy for the values of α and β. Another potential difficulty in measuring α is the curved nature of *S*-surfaces; however, α can be reliably measured from the relatively planar central part of the *S*-foliation be-

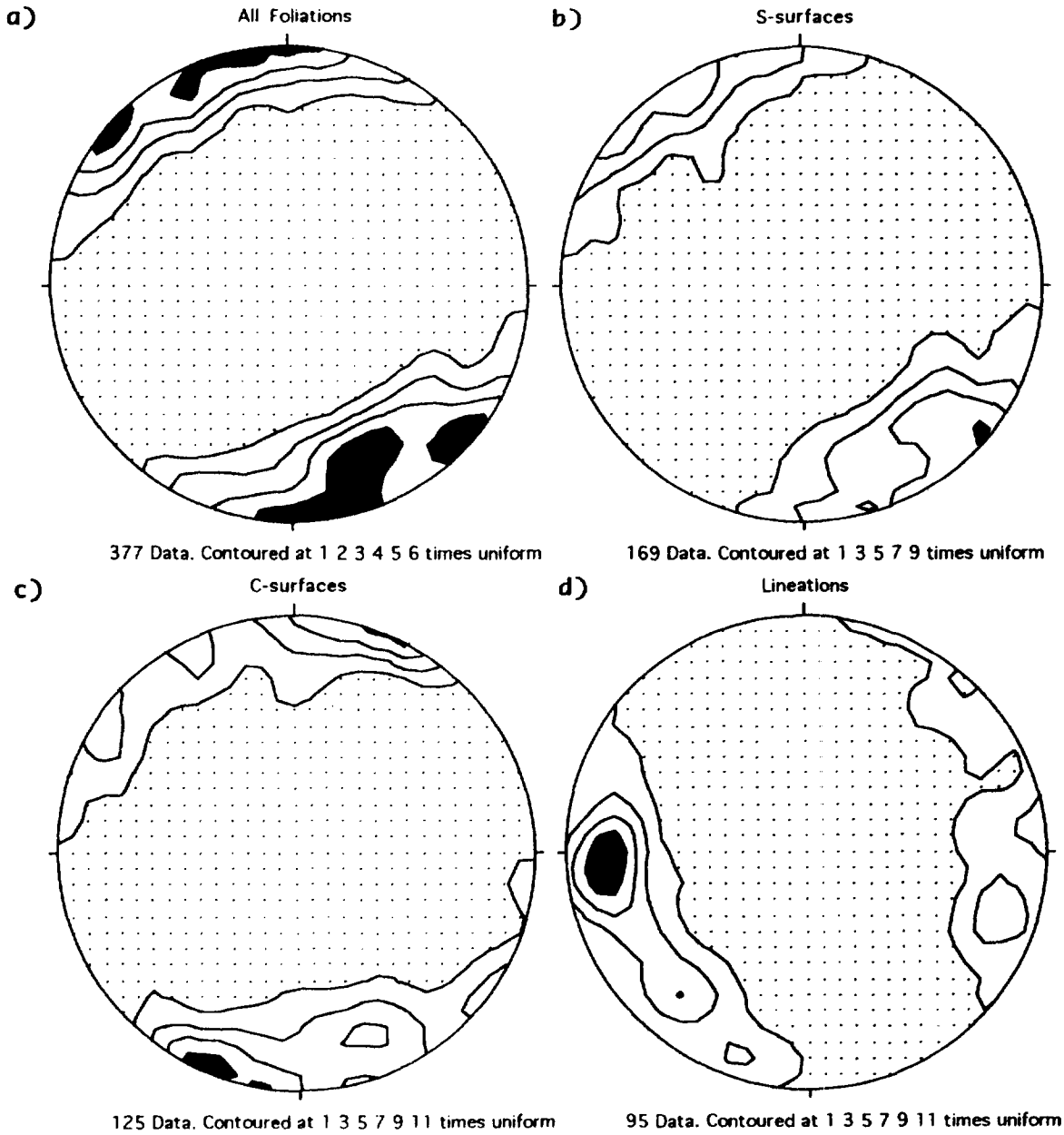

Fig. 4. Contoured stereoplots of poles to foliations and lineations in the Mushandike granite. All diagrams lower hemisphere equal area projections, contoured on the surface of the projection sphere by Stereoplot (Mancktelow 1989). Highest concentration of points in black, pole-free areas dotted. (a) All foliations measured in the Mushandike granite, including foliations outside shear zones that are not classified as *S*-, *C*-, or *C'*. (b) *S*-surfaces. (c) *C*- and *C'*-surfaces. (d) Lineations.

tween *C*- or *C'*-surfaces. This study emphasizes the more accurate measurements of δ, while α and β are estimated within a range of values.

All the shear zones have strong vertical or sub-vertical planar fabrics striking between N and E (Fig. 4a). Since most shear zones are dextral, the average strike of *C*- and *C'*-surfaces is clockwise to, or greater than, the average strike of *S*-surfaces (Figs. 4b & c). Many shear zones also contain a mineral lineation consisting of quartz rods, elongate quartz porphyroclasts, or phyllosilicates. The lineations are horizontal or subhorizontal, plunging gently to the west and locally southwest (Fig. 4d). All shear zone fabrics intensify to the south. Most show stronger planar than linear fabrics, but linear fabrics become relatively stronger towards the south.

S- and *C*- or *C'*-surfaces intersect in a line perpendicular, or at a high angle to, the shear direction, as defined by the lineation on *C*- or *C'*-surfaces. There is a considerable variation in morphology of the planar foliations which depends on four factors: (1) the angles α, β and δ, (2) the structures that define the *S*-surfaces, (3) the spacing of the *C*- or *C'*-surfaces, and (4) the relative strengths of *S*- and *C*- or *C'*-foliations. The first three factors are most diagnostic of the fabric type. It is

convenient to identify three end-member types, although most fabrics are intermediate between these end-members.

Porphyroclastic Type (Figs. 5a and 6a)

S-surfaces are defined by edges of quartz or feldspar porphyroclasts, which generally have sigmoidal shapes, with the edges of the porphyroclasts curving into C- or C'-surfaces. Porphyroclast shapes can be lensoid or quite irregular. C- or C'-surfaces are one to a few mm apart. α is typically 20–30°, and β is 0–5°, so that these are generally S–C rather than S–C' fabrics. α is approximately equal to δ. The average value of δ is 31° (24 measurements). The C- or C'-foliation is usually better developed than the S-foliation.

Megacrystic Type (Figs. 5b and 6b)

S-surfaces are defined by planar edges of feldspar megacrysts, which have rectangular or rhombohedral shapes in the plane normal to foliation. The width of the megacrysts (10–20 mm) defines the spacing between C'-surfaces. α is usually 30–40° and β is 5–10°. α is therefore less than δ, which has an average value of 42° (42 measurements). These are generally S–C' fabrics with C' stronger than S. Some megacrystic fabrics have very high values of α due to the shapes of the feldspar porphyroclasts that define S-surfaces.

Banded Type (Figs. 5c and 6c)

S-surfaces are defined by edges of quartz and muscovite bands several mm thick which curve into narrow C'-surfaces spaced 10–20 mm apart. Typical values of both α and β are from 15–25°. α is approximately equal to β and both are about half of δ, which has an average value of 38° (38 measurements). S is usually more prominent than C'.

The relations between α and β for the different fabric types are summarised in Fig. 7. A histogram of δ is shown in Fig. 8, with negative values assigned to fabrics where S-foliation is clockwise of C- or C'-foliation, indicating sinistral shear senses. There are no significant differences in the absolute values of δ between sinistral and dextral shear zones. The distribution is skewed towards lower absolute values. Greater positive or negative values clearly come from megacrystic and banded types, as observed in the field. A scatter diagram of absolute values of δ plotted against strike of shear zone is shown in Fig. 9, which shows a trend of decreasing δ with increasing strike. This geometry is consistent with a southward decrease of δ towards the MSZ. This trend can be confirmed within each type of fabric separately. The increase in shear zone density and the curvature of shear zone orientation towards parallelism with MSZ in the south of the Mushandike area show that bulk shear strain increases in this direction. The intensification of both planar and linear fabrics in shear zones together with the increasing predominance of L-fabrics suggest that strains within individual shear zones increase and thus become closer to plane strain to the south.

MICROSTRUCTURES

The essential microstructural features of all the shear zones are due to crystal plasticity of quartz and the breakdown of feldspar to muscovite which may cause a volumetric component of strain. Porphyroclastic fabrics have sigmoidal (σ-type, Passchier & Simpson 1986) or elliptical porphyroclasts of quartz, or sometimes feldspar, 5 mm long, composed of original grains about 0.3 mm long which have a moderate grain shape fabric, undulose extinction, deformation bands, and serrated grain boundaries (Fig. 10a). Asymmetric tails on porphyroclasts consist of much finer (0.03 mm) recrystallized quartz grains. A few mica fish are seen, which have been sheared along basal cleavage planes where these are parallel to the C-foliation. The matrix consists of very fine grained muscovite which anastomoses around porphyroclasts and fish. S-surfaces are defined by edges of porphyroclasts and the grain shapes of individual quartz grains within them, while C-surfaces are defined by narrow zones (0.1 mm) of very fine grained muscovite.

The megacrystic fabric consists of rectangular or rhombohedral plagioclase, orthoclase or perthite megacrysts, which are pervasively altered to very fine-grained sericite, particularly in the case of plagioclase grains. Recrystallization of K-feldspar megacrysts to small equant grains of quartz and alkali feldspar (0.03 mm) occurred along their margins (Fig. 10b). Ribbons of elongate quartz grains with serrated margins are parallel to the megacryst margins. Fine-grained quartz, feldspar, muscovite, chlorite and sericite comprise the matrix, which has a much lower proportion of phyllosilicates than the porphyroclastic type. S-surfaces are defined by the straight edges of feldspar megacrysts, as well as quartz ribbons and individual quartz grain shapes. C- or C'-surfaces are defined by zones of similar size to those in the porphyroclastic type, but are filled mainly by very fine-grained quartz rather than muscovite.

The most prominent microstructure of the banded fabrics are sigmoidal ribbons of both quartz and feldspar from 0.5 mm to several cm long and 0.5 mm–1 cm wide (Fig. 10c). Quartz grains within the ribbons are 0.3 mm long and have a good shape fabric, serrated grain boundaries, and deformation bands that are commonly orientated sub-perpendicular to the edges of the ribbons. Feldspar grains are 0.4–0.5 mm. Ribbons are separated by bands of fine-grained muscovite 0.5 mm wide, with abundant kink bands. S-surfaces are defined by the relatively straight section of ribbon boundaries near the inflexion point, and quartz grain shapes. C'-surfaces are narrow zones or surfaces of shear with rather variable values of β, along which recrystallization of quartz occurs to a finer grain size (Fig. 10c).

A crucial feature of all types of fabric is the difference between S- and C- or C'-surfaces. C- or C'-surfaces are

always planar and show evidence for localized shear displacement from deformation of *S*-surfaces (Fig. 10) and shearing of muscovite along basal planes. Higher strain (or a higher rate of recrystallization) on *C*- and *C'*-surfaces is shown by a higher proportion of fine, dynamically-recrystallized grains along these surfaces (Fig. 10). In contrast, *S*-surfaces are curved and never displace *C*- or *C'*-surfaces, even when the *S*-surfaces are confined to the edges of rigid feldspar porphyroclasts or megacrysts (Figs. 10a & b). Muscovite laths parallel to *S*-surfaces are never sheared synthetically to the overall sense of shear, but occasionally they are sheared antithetically, in a geometry similar to that illustrated for mica fish by Lister & Snoke (1984). Therefore synthetic shear has not occurred on *S*-surfaces, even by infinitesimal displacement along pervasive shears, because this would be visible from deformation of *C*- or *C'*-surfaces around rigid porphyroclasts.

DISCUSSION

Theories for development and orientation of planar fabrics

Platt & Vissers (1980) suggested that shear bands form by the development of shears (*C*- or *C'*-planes) close to the direction of maximum shear strain rate (slip lines), during deformation of materials with a pre-existing anisotropy which defines the *S*-foliation. White *et al.* (1980) also concluded that shear bands develop as a consequence of anisotropy formed in an earlier stage of deformation. A single set of shear bands at a low angle to the shear plane and with a fixed angle to an internal *S*-foliation would form in the simple example of non-coaxial deformation given by Platt & Vissers (1980). The spread of δ and its systematic variation (Figs. 8 and 9) suggests that shears did not develop along surfaces of maximum shear strain with a fixed value of δ in the Mushandike fabrics.

Platt (1984) suggested that shear bands or extensional crenulation cleavages form due to flow partitioning in a zone of overall simple shear. Slip may occur along single sets of discrete surfaces parallel to *S*-foliation which separate domains of stretching parallel to *S*-foliation. The *ecc* and the *S*-foliation rotate towards the shear plane. However, there is no evidence for extensive shear on surfaces parallel to *S*-foliation on any scale in the fabrics described here (see above), although it is not possible to completely rule out some slip on rare surfaces parallel to *S*, or coaxial stretching parallel to *S*-foliation. Alternatively, slip may occur along *ecc*-surfaces with shortening parallel to the *ecc*, which rotates away from the shear plane with progressive shear. The observation that β does not change systematically towards the MSZ in any single type of shear zone fabric suggests that *C'*-surfaces did not rotate with increasing strain. This is also suggested by the planar nature of *C'*-surfaces: if significant rotations occurred in a material with discontinuous *C'*-surfaces, strain incompatibilities would distort initially planar surfaces, as observed experimentally by Shimamoto (1989). There is some evidence that neither of Platts' two models, or intermediate situations, may apply to these fabrics. Likewise, lack of synthetic shear on *S*-surfaces suggests that the Mushandike shear zone fabrics did not form in the manner demonstrated by Dennis & Secor (1987, 1990).

An alternative model for these shear zone fabrics starts by considering that *S*-surfaces lie parallel to the *XY* plane of the local finite strain ellipsoid, and that *C*-surfaces are zones of concentrated strain. The local finite strain ellipsoid represents the strain in domains between *C*-surfaces, which are separated by a few millimetres. The total shear strain will therefore be the sum of a simple shear in domains between *C*-surfaces, and a concentrated shear along the *C*-surfaces themselves. α will follow the familiar relationship:

$$\tan 2\alpha = -2/\gamma$$

where γ is the simple shear in these domains (cf. Ramsay 1967, 1980). This model assumes that there is no shear parallel to *S*-surfaces, and that *C*-surfaces will be parallel to the shear plane. This simplest case is similar to the model of Berthé *et al.* (1979). We believe that this simple account of *S*-surfaces is appropriate to most of the fabrics described here, firstly because *S*-surfaces within the shear zones are identical in appearance and continuous with foliations adjacent to shear zones in foliated granite. Secondly, slip did not occur on *S*-surfaces. Thirdly, the intersection between *S*- and *C*- or between *S*- and *C'*-surfaces is perpendicular or at a high angle to the stretching lineation, indicating that little slip occurred oblique to the shear direction, and that *S*-surfaces can therefore be parallel to the local *XY* plane. Finally, long axes of deformed quartz grains, which can be assumed to be parallel to the *X*-axis of the local finite strain ellipsoid, are also parallel to the *S*-foliation in sections perpendicular to the foliation and parallel to the lineation.

We extend the simplest case of *S*- and *C*-surfaces to include *C'*-surfaces, which are also zones of concentrated strain, but inclined to the shear plane at an angle β. We suggest that the *S*-surfaces also follow the *XY* planes of the local finite strain ellipsoid in domains of simple shear between *C'*-surfaces. δ will therefore also have the same relationship to γ as that given above for α. β is commonly 15–25° in banded fabrics, and *C'*-surfaces are therefore geometrically analogous to Riedel shears observed in simple shear experiments and fault gouges (e.g. Rutter *et al.* 1986) and in strike-slip fault systems (e.g. Sylvester 1988). The geometrical similarity between shear surfaces in 'brittle fault zones' and *S–C* mylonites has been noted by Evans & Dresden (1991). Pursuing this analogy further, we suggest that *C'*-surfaces form in the orientation of a Coulomb failure surface at an angle of less than 45° to the maximum principal stress. *C'*-surfaces and these values of β are common when there is large mechanical anisotropy in shear zones with banded fabrics. The precise orientation of *C'*-surfaces will be affected by the anisotropy, which

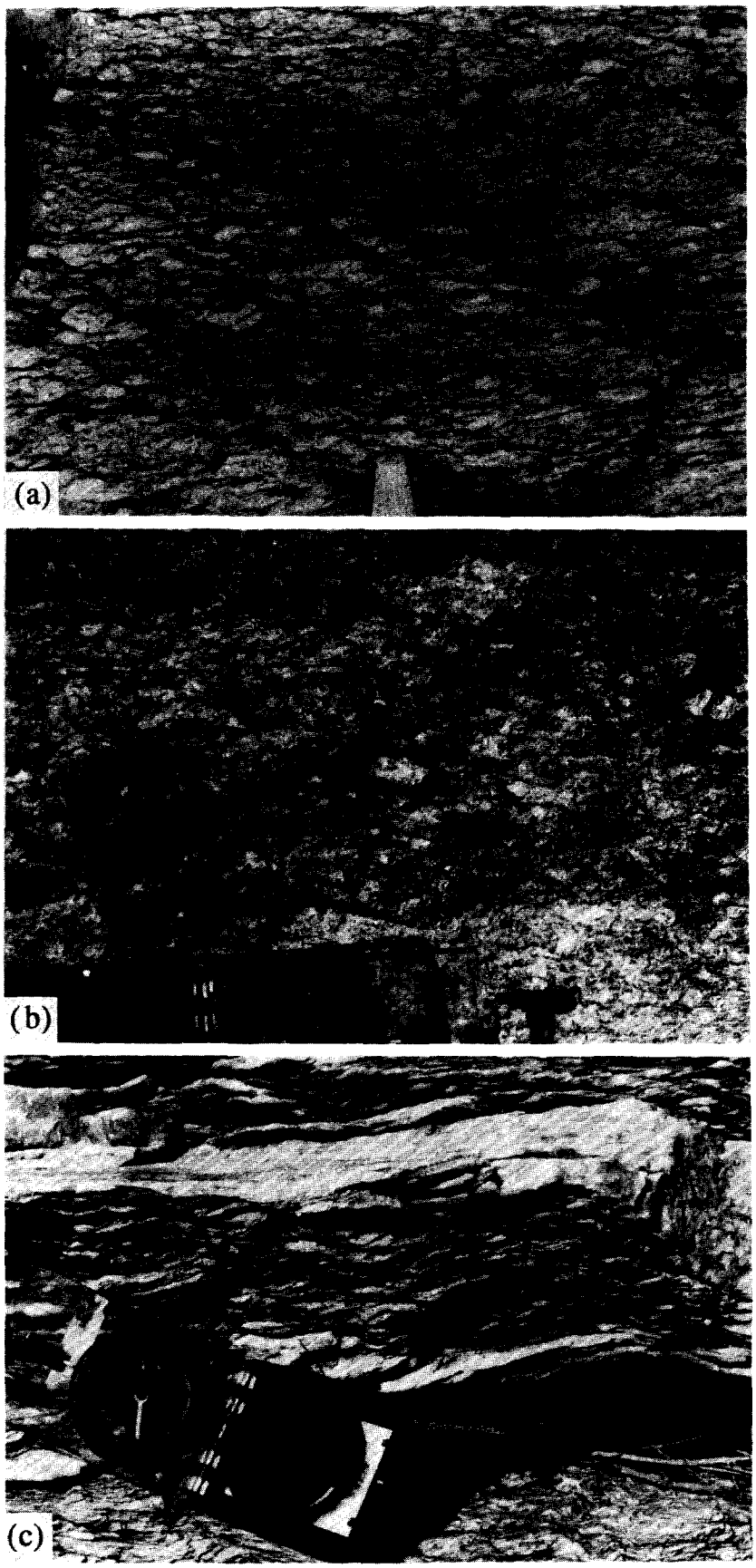

Fig. 5. *S–C* and *S–C′* fabrics in shear zones in the Mushandike granite. All photographs are perpendicular to *S*, *C*, or *C′* and parallel to lineation, and show dextral shear sense. The shear zone boundaries are horizontal. (a) Porphyroclastic type. Diameter of pen is 10 mm. (b) Megacrystic type. (c) Banded type.

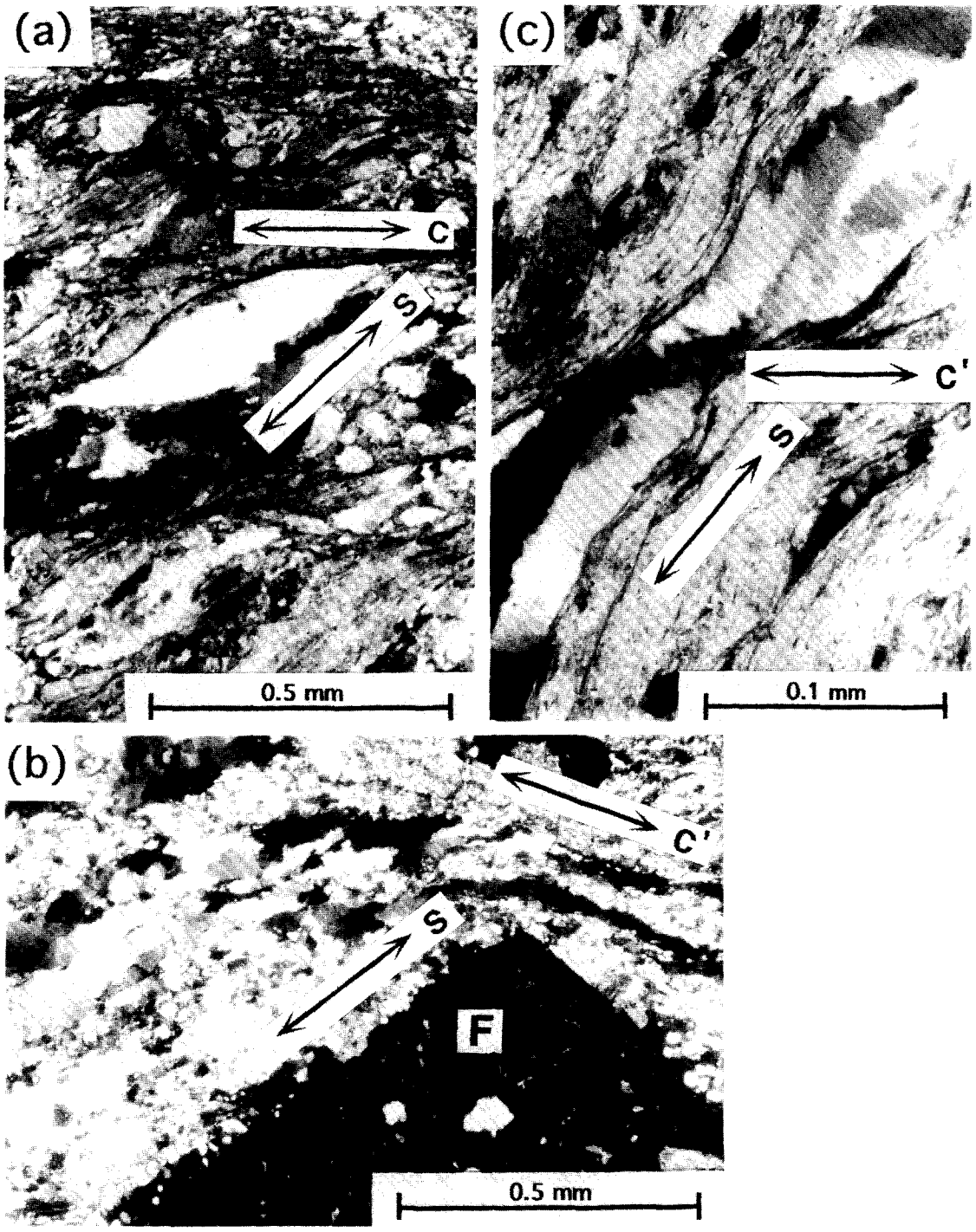

Fig. 10. Microstructures of typical examples of fabrics in the Mushandike shear zones. All sections are perpendicular to S, C, or C' and parallel to lineation, and show dextral shear sense. (a) Porphyroclastic fabric showing σ-type asymmetrical tail. (b) Megacrystic fabric. Feldspar megacryst (F) controls the orientation of S- and C'-surfaces. Recrystallization of the megacryst can be seen on the face parallel to S. (c) Banded fabric, showing a quartz band surrounded by muscovite bands. Quartz is recrystallizing to a fine grain size along the C'-surface.

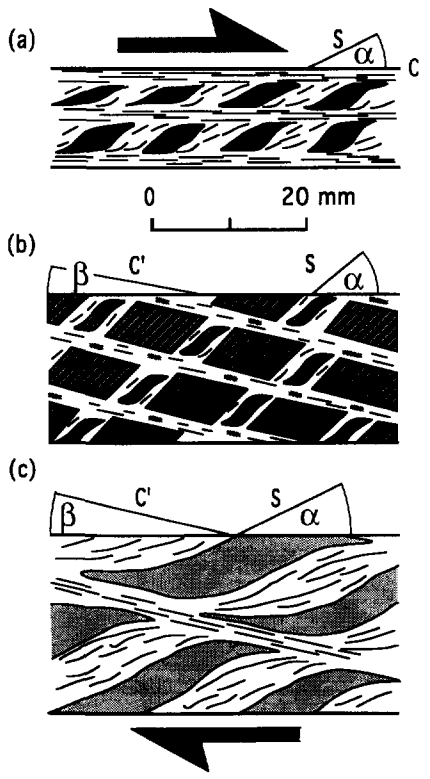

Fig. 6. Schematic diagrams of S–C and S–C' fabrics in shear zones in the Mushandike granite. (a) Porphyroclastic type. (b) Megacrystic type. (c) Banded type.

may explain the difference in β values between the megacrystic and banded fabrics. Control of shear band orientation by anisotropy was suggested by Passchier (1984) for his type II and type III shear bands. Coulomb failure may not, however, be an adequate explanation for all C'-foliation, since C'-foliation is observed in rocks deformed under amphibolite facies conditions. Although the behaviour of C'-surfaces with strain is not clear, the evidence presented above suggests that they have not rotated significantly with strain.

There is some additional evidence that C'-foliation forms in a different way from C-foliation. C-foliations contain both quartz and muscovite, while the C'-foliations contain only quartz. This implies large changes from the initial granite composition in the formation of C'-foliation, which could occur by local volume-loss removal of all phases except quartz, or by local volume increase by addition of quartz, or some combination of these two that could be isovolumetric. Chemical evidence for volume increase during formation of extensional crenulation cleavages was reported by Behrmann (1984).

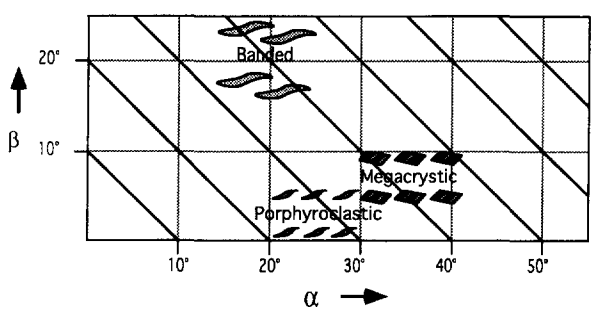

Fig. 7. Approximate range of α and β values for porphyroclastic, megacrystic, and banded types of fabric. The range of values for each type is indicated by the area covered by the relevant symbol. Diagonal lines are lines of constant δ.

The model for the formation of these fabrics thus consists of S-foliation forming parallel to the XY plane of the local finite strain ellipsoid in between discrete shears that are either parallel to the shear zone boundaries (C-foliation) or slightly oblique (C'-foliation). C'-foliation forms in the orientation of Riedel shears, and may be influenced by anisotropy. This model differs from several others (e.g. Burg 1987, Ghisetti 1987, Berthé *et al.* 1979) by combing the explicit recognition that the S-foliation reflects a *local* finite strain in volumes between discrete shears with an account of the formation of C'-surfaces. The total finite strain must also include the contribution of strain on the discrete shears, C or C'.

This model predicts that the value of δ decreases as γ increases in domains between C-surfaces or C'-surfaces increases. Figure 9 shows that δ decreases, largely due to a decrease in α, as shear zone strike approaches the strike of MSZ, towards the south of the Mushandike granite. Higher shear strains on individual shear zones towards the south are inferred from more intense S- and C- or C'-foliations in these shear zones. The field evidence therefore suggests that at least part of the higher total finite strain in the shear zones is due to rotation of the S-foliation between C- or C'-shears and an increase in local strain in these domains. A detailed analysis of this would require bulk and local strain measurements, which cannot be made because there are no suitable strain markers.

Slip on C'-surfaces cannot accumulate while preserving overall simple shear unless some compensating mechanism operates. Although it is attractive to confine models to overall simple shear, the discontinuous geometry of the shear zones, separated by foliated granite, suggests that shear zones may not evolve as continuous zones of simple shear. They may have an en échelon geometry, or become separated along subsequent shears (Fig. 3). A non-simple shear model of shear band evolution has been also suggested by Passchier (1991), who maintains that shear bands rotate towards the shear plane and contribute a component of extension parallel to the shear zone.

The model must be modified for low strain states of megacrystic fabrics. In these fabrics, the orientation of S-surfaces is controlled by faces of rectangular or rhombohedral feldspar megacrysts which have one pair of faces parallel to C'-surfaces and the other pair subperpendicular to C'-surfaces in the section perpendicular to foliation and parallel to the shear direction (Fig. 6b). This geometry gives large δ values, which may decrease with strain because α decreases as recrystallization of feldspars occurs.

Questions about the timing of formation of foliations in shear zones have provoked considerable discussion (e.g. Lister & Snoke 1984). Because C- and C'-foliations

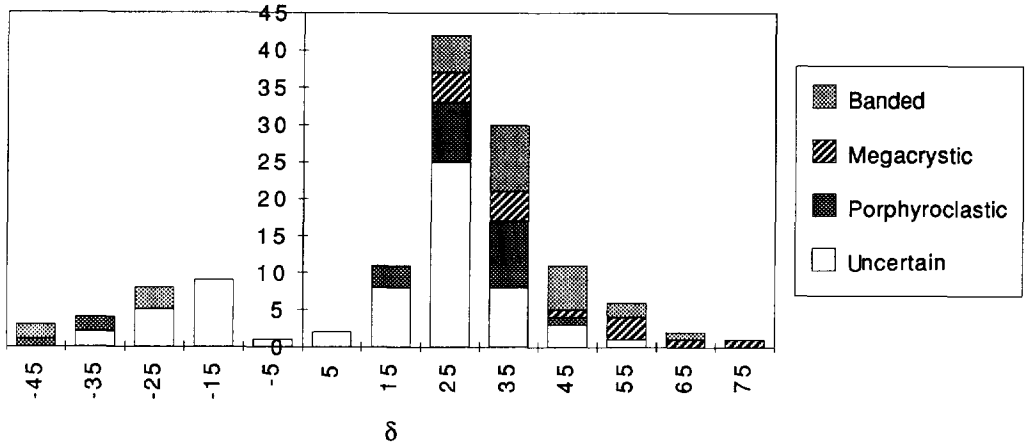

Fig. 8. Histogram of δ subdivided by type of fabric. Negative values are for S-surfaces anticlockwise of C- or C'-surfaces indicating sinistral shear sense. Measurements made before the classification was devised are included in the 'uncertain' category.

are always and exclusively restricted to shear zones where S-foliations are also intense, it is likely that S-, C- and C'-foliations in the Mushandike shear zones belong to a single progressive deformation. Furthermore, the orientation of C- and C'-foliations changes sympathetically with S-surfaces, suggesting that they are not a later regional overprint. Mineral assemblages, deformation mechanisms and deformation conditions are common to S-, C- and C'-surfaces, also indicating that they formed coevally (cf. Burg 1987). None of the models discussed here considers the complications introduced by reactivation of structures as discussed in detail by Lister & Snoke (1984). Reactivation may be an additional reason for differences in interpretation of S–C and S–C' fabrics.

Comparison of Mushandike fabrics with other field-based studies

Most of the Mushandike fabrics are closer to the type I category of Lister & Snoke (1984) because continuity is often preserved across C-surfaces, and few large mica fish, which characterize type II fabrics, are observed. However, the relative strengths of S- and C- or C'-foliations are variable and therefore the fabrics do not easily fall into the Lister & Snoke classification, in which type I fabrics have stronger S-surfaces. Other recent descriptions of shear zone fabrics have similarities with the results reported here. Examples of fabrics which appear similar to our porphyroclastic type include the C–S fabrics of Balé & Brun (1989) and the fabrics described by Stuart-Smith (1990). Tyler & Griffin (1990) show a fabric in their fig. 4(e) which is very similar to our megacrystic type, and the C'–S fabrics of Balé & Brun (1989) and fabrics described by Culshaw (1991) have strong similarities with our banded type.

Numerous studies have reported a decrease in δ with strain as observed here (e.g. Zee *et al.* 1985, Burg 1987, Ghisetti 1987, Balé & Brun 1989, Scheuber & Andriessen 1990, Rykkelid & Fossen 1992). Burg (1987) and Ghisetti (1987) treated the S-foliation as the XY plane of the finite strain ellipsoid. The difference between these studies together with this report, and the models and observations of Platt & Vissers (1980), Platt (1984) and Dennis & Secor (1987,1990), in which slip occurs on S-surfaces may reflect the fact that different fabrics form and evolve in different ways. A single model is probably inadequate to describe all shear zone fabrics, even though they may have apparent similarities.

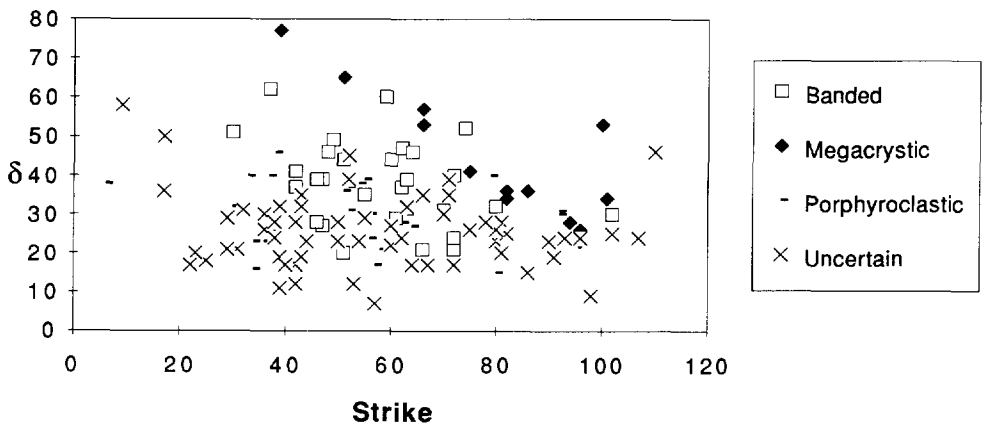

Fig. 9. Absolute values of δ plotted against the strike of the S-surface for each type of fabric.

Experimental investigations of shear zone fabrics

Shear bands were developed experimentally in ice-mica models by Wilson (1984). The experiments show that differentiation can develop as a result of mechanical processes involving early shear sub-parallel to a pre-existing foliation, and rotation of the foliation into the XY plane of the bulk strain ellipsoid. The latter process was also described from experiments on KCl/mica schists deformed in simple shear by Williams & Price (1990) and may be relevant to the formation of banded fabrics.

Simple shear experiments on cooking salt by Shimamoto (1989) have considerable relevance to this study because of the experimental geometry, and because both halite and undeformed Mushandike granite have isotropic textures. In the experiments, an S-foliation formed parallel to the XY plane (as also observed in experimentally deformed quartzites by Dell'Angelo & Tullis 1989), and after a critical shear strain, localization occurred on Riedel (R1) and Y shears. R1 shears formed in the predicted Coulomb failure orientation. Shears were rotated and distorted by subsequent deformation. The formation and orientation of foliation parallel to the XY plane and the formation of R1 shears in the predicted Coulomb orientation in these experiments correspond with the predictions of our model, and lend additional support to the model because the experiments are based on simple shear of an initially isotropic material.

CONCLUSIONS

S–C and S–C' fabrics can be described by the angles α, β and δ (Fig. 1). Using these parameters, fabrics in small dextral shear zones in the Mushandike area of the Zimbabwe Archaean craton can be classified into *porphyroclastic*, *megacrystic*, and *banded types* (Fig. 7). This classification seems to be applicable to several other recent descriptions of S–C and S–C' fabrics from field examples and experiments, and a plot of α vs β such as Fig. 7 summarizes the classification. Variations in the values of α, β and δ are controlled by both strain and microstructure. δ decreases with strain in all types.

We have found some evidence that several previous theories for S–C and S–C' fabrics do not fit the Mushandike fabrics. Instead, we suggest that S-surfaces lie parallel to the XY plane of the local finite strain ellipsoid in domains between discrete shear on C- or C'-surfaces. C'-surfaces may form as Riedel shears in the orientation of a Coulomb failure surface in a simple shear zone, and their development may be controlled by anisotropy. The way in which C'-surfaces evolve with strain is uncertain, but there is some evidence that their orientation does not change significantly. Increase in total strain on shear zones in the Mushandike area is at least partly accommodated by rotation of S-surfaces with the local finite strain ellipsoid in domains between C- or C'-surfaces. This model accounts satisfactorily for the main features of the fabrics observed in this study, although in view of the evidence from other studies, S–C and S–C' fabrics may form in more than one way.

Acknowledgements—We respect the memory of Thorley Sweetman who participated in much of the fieldwork at Mushandike Game Reserve. We are grateful for detailed comments from John Platt, Deepak Srivastava, Graham Park, and Jan Behrmann. Field work was sponsored by University of Zimbabwe grant 2.9999.10/3347. We are grateful to the department of National Parks and Wild Life Management, particularly at Mushandike Game Reserve, and to the staff at the Department of Geology, University of Zimbabwe, for their cooperation. PJT acknowledges a travel grant from the Royal Society of London.

REFERENCES

Balé, P. & Brun, J.-P. 1989. Late Precambrian thrust and wrench zones in northern Brittany. *J. Struct. Geol.* **11**, 391–405.

Behrmann, J. H. 1984. A study of white mica microstructure and microchemistry in a low grade mylonite. *J. Struct. Geol.* **6**, 283–292.

Behrmann, J. H. 1987. A precautionary note on shear bands as kinematic indicators. *J. Struct. Geol.* **9**, 659–666.

Berthé, D., Choukroune, P. & Jegouzo, P. 1979. Orthogneiss, mylonite and non-coaxial deformation of granites: the example of the South Armorican Shear Zone. *J. Struct. Geol.* **1**, 31–24.

Blenkinsop, T. G., Dhilwayo, J. & Muranda, S. C. 1990. Intracratonic shearing on shear zones of the Mushandike granite, Zimbabwe. *Proceedings of the Second Symposium of Science and Technology, Research Council of Zimbabwe*. Vol. IIA, Research Council of Zimbabwe, 396–421.

Burg, J. P. 1987. Regional shear variation in relation to diapirism and folding. *J. Struct. Geol.* **9**, 925–934.

Culshaw, N. 1991. Post-collisional oblique convergence along the Thelon Tectonic Zone, north of the Bathurst Fault, NWT, Canada. *J. Struct. Geol.* **13**, 501–506.

Dell'Angelo, L. N. & Tullis, J. 1989. Fabric development in experimentally sheared quartzites. *Tectonophysics* **169**, 1–21.

Dennis, A. J. & Secor, D. T. 1987. A model for the development of crenulations in shear zones with applications form the southern Appalachian piedmont. *J. Struct. Geol.* **9**, 809–817.

Dennis, A. J. & Secor, D. T. Jr. 1990. On resolving shear direction in foliated rocks deformed by simple shear. *Bull. geol. Soc. Am.* **102**, 1257–1267.

Dhilwayo, J. 1990. The geometry, kinematics and dynamics of Mushandike shear zones (eastern section). Unpublished B.Sc. Hons. thesis, University of Zimbabwe.

Evans, B. & Dresden, G. 1991. Deformation of earth materials: six easy pieces. Contributions in Tectonophysics, U.S. National Report to International Union of Geodesy and Geophysics, 1987–1990. Am. Geophys. Union, 823–843.

Ghisetti, F. 1987. Mechanisms of thrust faulting in the Gran Sasso chain, central Appenines, Italy. *J. Struct. Geol.* **9**, 955–967.

James, P. R. 1975. A deformation study across the northern margin of the Limpopo Belt, Rhodesia. Unpublished Ph.D. thesis, University of Leeds.

Lister, G. S. & Snoke, A. W. 1984. *S–C* Mylonites. *J. Struct. Geol.* **6**, 617–638.

Moorbath, S., Taylor, P. N., Orpen, J. L., Treloar, P. & Wilson, J. F. 1987. First direct radiometric dating of Archaean stromatolitic limestone. *Nature* **326**, 865–867.

Muranda, S. C. M. 1990. The geology of the Mushandike area with particular emphasis on shear zones: geometry and strain integration, displacements and synkinematic history. Unpublished B.Sc. Hons. thesis, University of Zimbabwe.

Mancktelow, N. 1989. Stereoplot. A programme for plotting and analysis of directional data.

Passchier, C. W. 1984. The generation of ductile and brittle shear bands in a low-angle mylonite zone. *J. Struct. Geol.* **6**, 273–281.

Passchier, C. W. 1991. Geometric constraints on the development of shear bands in rocks. *Geol. en Mijnb.* **70**, 203–211.

Passchier, C. W. & Simpson, C. 1986. Porphyroclast systems as kinematic indicators. *J. Struct. Geol.* **8**, 831–843.

Platt, J. P. 1984. Secondary cleavages in ductile shear zones. *J. Struct. Geol.* **6**, 439–442.

Platt, J. P. & Vissers, R. L. M. 1980. Extensional structures in anisotropic rocks. *J. Struct. Geol.* **2**, 397–410.

Ramsay, J. G. 1967. *Folding and Fracturing of Rocks*. McGraw Hill, New York.

Ramsay, J. G. 1980. Shear zone geometry: a review. *J. Struct. Geol.* **2**, 83–89.

Rutter, E. H., Maddock, R. H., Hall, S. H. & White, S. H. 1986. Comparative microstructures of natural and experimentally produced clay-bearing fault gouges. *Pure & Appl. Geophys.* **124**, 3–30.

Rykkelid, E. & Fossen, H. 1992. Composite fabrics in mid-crustal gneisses: observations from the Oygarden Complex, West Norway Caledonides. *J. Struct. Geol.* **14**, 1–10.

Scheuber, E. & Andriessen, P.A.M. 1990. The kinematic and geodynamic significance of the Atacama fault zone, northern Chile. *J. Struct. Geol.* **12**, 243–257.

Shimamoto, T. 1989. The origin of *S–C* mylonites and a new fault-zone model. *J. Struct. Geol.* **11**, 51–64.

Simpson, C. 1986. Determination of movement sense in mylonites. *J. Geol. Education* **34**, 246–261.

Simpson, C. & Schmid, S. 1983. An evaluation of criteria to deduce the sense of movement in sheared rocks. *Bull. geol. Soc. Am.* **94**, 1281–1288.

Stuart-Smith, P. G. 1990. The emplacement and fault history of the Coolac Serpentinite, Lachlan Fold Belt, southeastern Australia. *J. Struct. Geol.* **12**, 621–638.

Sylvester, A. G. 1988. Strike-slip faults. *Bull. geol. Soc. Am.* **100**, 1666–1703.

Tyler, I. M. & Griffin, T. J. 1990. Structural development of the King Leopold Orogen, Kimberley region, Western Australia. *J. Struct. Geol.* **12**, 703–714.

White, S. H., Burrows, S. E., Carreras, J., Shaw, N. D. & Humphreys, F. J. 1980. On mylonites in ductile shear zones. *J. Struct. Geol.* **2**, 175–187.

Williams, P. F. & Price, G. P. 1990. Origin of kinkbands and shear-band cleavage in shear zones: an experimental study. *J. Struct. Geol.* **12**, 145–164.

Wilson, C. J. 1984. Shear bands, crenulations and differentiated layering in ice-mica models. *J. Struct. Geol.* **6**, 303–320.

Wilson, J. F. 1968. The geology of the country around Mashaba. *Bull. Rhod. Geol. Sur.* **68**.

Wilson, J. F. 1990. A craton and its cracks: some of the behaviour of the Zimbabwe block from the late Archean to the Mesozoic in response to horizontal movements, and the significance of some of its mafic dyke fracture patterns. *J. Af. Earth Sci.* **10**, 483–501.

Zee, R. Y. S., Teyssier, C., Hobbs, B. E. & Ord, A. 1985. Development of foliations in the Wyangala Gneiss, Central New South Wales, Australia. Abstract. *J. Struct. Geol.* **7**, 501.